

페이딩 매질에서 대역확산  
주파수도약 통신시스템의 전송특성  
Transmission Characteristics of  
FFH-SS Communication System  
in Fading Media

\* 김 원 후(Kim, W. H.)

\*\* 전 계 석(Jun, K. S.)

요 약

이 논문은 시간 및 주파수 선택성페이딩이 동시에 존재하는 채널에서 대역확산 주파수 도약통신시스템의 전송특성을 제시한다. 수신기는 승적합산기를 포함한 binary noncoherent matched-filter fast FH-SS 시스템이다. 이 시스템에서 SNR, 채널 선택도, 전력비 등의 변동에 따른 오차확률은 데이터율을 고려하지 않고 다이버시티 개념을 사용하여 구하였으며, 오차확률에 대한 데이터를 분석한 결과 FH-SS 시스템은 시간 선택성 페이딩 채널에서 전송특성이 우수함을 나타내었다.

ABSTRACT

In this paper, the transmission characteristics of a frequency-hopped spread spectrum communication system operating in the presence of both time and frequency-selective fading channel is presented. The receiver is a binary noncoherent matched-filter FFH-SS system with square-law combiner. The probability of error to the variations of the parameters such as signal-to-noise ratio, selectivity of a chan-

\* 한국항공대학교 전자공학과 교수  
\*\* 경희대학교 전자공학과 교수

nel, and power ratio is derived with the use of diversity concept without considering the data rate. The analysis of the data for probability of error shows that the performance of FFH-SS system in time-selective fading channel is better than in frequency-selective fading channel.

## I. INTRODUCTION

Since about the mid-1950's the spread spectrum systems have been developed primarily for military antijamming tactical communications, guidance systems, and antimultipath system (1), etc. Recently, Cooper and Nettleton (2) proposed a spread spectrum system for cellular mobile communication and presented some results that the spectrum efficiency and the flexibility of the system were superior to the conventional techniques, for example, the frequency division multiple-access(FDMA) with frequency modulation.

Gardner et al. (3), and Borth et al. (4) analyzed the effects of fading for direct sequence systems, and Milstein et al. (5) and Geraniotis et al. (6) for frequency hopping systems with strict assumptions and approximations.

In this paper, the performance of noncoherent frequency hopped spread spectrum

communication systems over general fading dispersive channels, is presented in terms of the probability of error as a performance measure.

## II. CHANNEL CHARACTERIZATION

The type of fading considered in this paper is Rician or specular-plus-Rayleigh fading (7) (8). That is, for a single transmitted signal, the received signal consists of a replica of the transmitted signal plus a weaker Rayleigh-faded version of this signal. This will be the situation whenever the transmission medium is such that there is a strong path and a number of weak paths.

The mechanism that the fading effects occur is shown in Fig. 1, where the differences in propagation path cause the differences in relative propagation delay, hence the frequency selectivity, and the relative movement of transmitter and/or receiver or scatterer cause the Doppler shift, hence the time selectivity.

A systematic model of a Rician channel is shown in Fig. 2, where the channel is the parallel combination of a deterministic and a random time-varian linear filters.

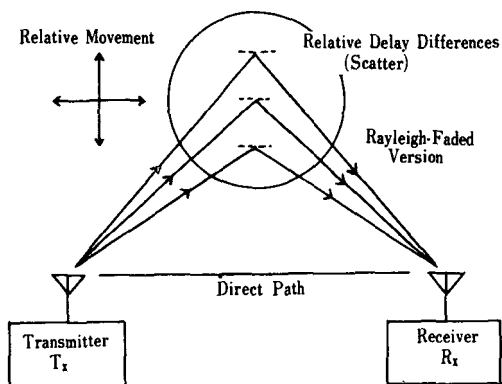


Fig.1 Mechanization of a Rician Fading Channel.

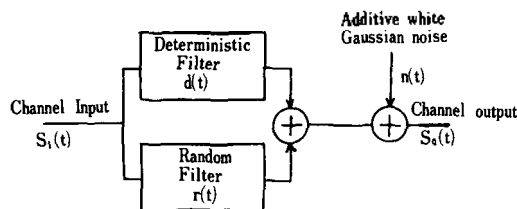


Fig.2 Systematic Model of a Rician channel.

The input complex signal  $s_i(t)$  feeds to both filters. The output of the deterministic filter  $d(t)$ , the output of the random filter  $r(t)$ , and a Gaussian additive noise  $n(t)$  are combined to form  $S_o(t)$ , the complex signal of the channel output.

### III. BINARY FFH-SS COMMUNICATION SYSTEM MODELS

#### 3-1. Transmitter Model

The transmitter for the binary noncoherent fast frequency-hopped spread spectrum (9) signal is shown in Fig. 3. The data signal of  $d(t)$  is a sequence of positive and negative rectangular pulses of duration  $T$ . The amplitude of the  $l$ th pulse is denoted by  $d_l$  for  $lT \leq t < (l+1)T$ , and  $d_l$  is either  $+1$  or  $-1$  for each  $l$ .

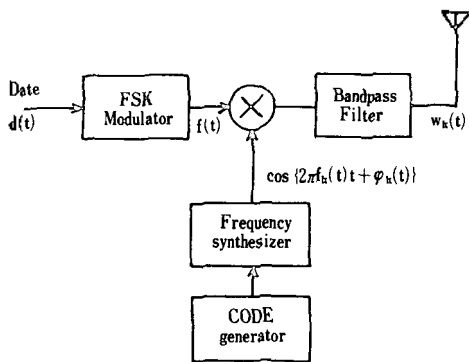


Fig.3 Binary FFH-SS Transmitter Model.

The data signal  $d(t)$  is the input to a FSK modulator, and the corresponding output is

$$f(t) = \cos \{ (2f_c + d(t)\Delta f)t + \theta(t) \} \quad (3-1)$$

where  $f_c$  is the carrier frequency,  $f$  is one-half the spacing between the two tone frequencies, and  $\theta(t)$  is the phase introduced by the

FSK modulator. For the simplicity of analyses, it is assumed that the two FSK tones are orthogonal, i.e.,

$$\Delta f = \frac{n}{T} \quad \text{for positive integer } n \quad (3-2)$$

However the analyses can be easily extended for non-orthogonal cases with the aid of correlation coefficient between the signaling alphabets.

#### 3-2. Receiver Model

A block diagram for a binary fast frequency-hopped spread spectrum communication system with incoherent matched-filters is shown in Fig. 4. Apart from a phase shift, two matched-filters are matched to one of the two possible waveforms that are successively repeated to form the transmitted binary signal. Assuming the code at the receiver is synchronized to that at the transmitter, the input signal to the matched-filters is an ordinary FSK modulated signal. The outputs of the matched-filters are envelope detected by the square-law detector and subtracted for bit decision. Diversity combining is performed by accumulating the successive  $L$  hops of an information. When the hops are bit interleaved, some delay and summing circuits are required. (10)

The dehopped signal, neglecting the higher frequency components, is

$$S_k(t) = R_o \{ X_k(t) \exp(j2\pi f_c t) \} \quad (3-3)$$

$$1 \leq k \leq L$$

where

$$X_k(t) = \sqrt{\frac{E}{2T_k}} \exp \{ j2\pi(d(t)\Delta f + \phi_k(t) + \phi'_k(t) + \phi_k(t)) \}$$

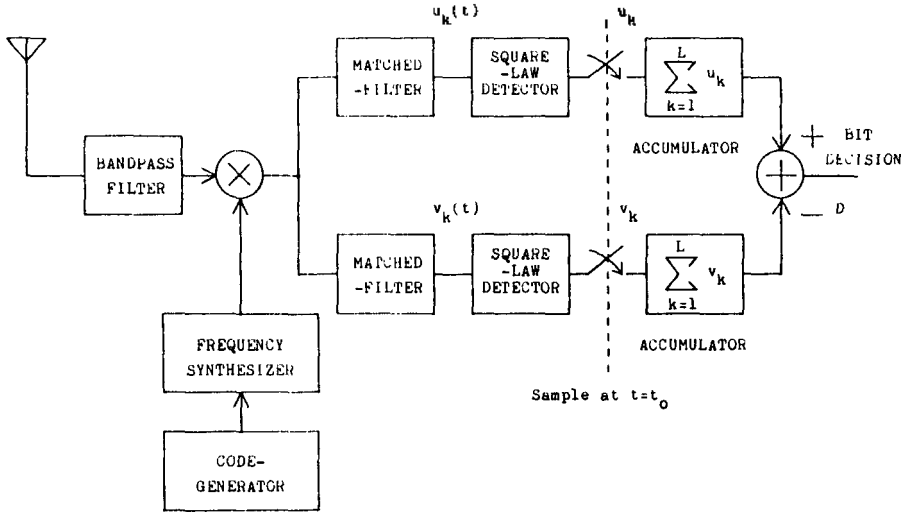


Fig.4 Binary FFH-SS Receiver Model.

and the  $\varphi'_k(t)$  is the phase of the dehopper at the receiver which has identical statistics to  $\varphi_k(t)$ .

#### IV. DERIVATION FOR THE PROBABILITY OF ERROR

The output at the  $k$ th hop period is

$$d_k = |u_k|^2 - |v_k|^2 \tag{4-1}$$

Where  $u_k$ , and  $v_k$  are the matched-filter outputs at the sampling instant, (11) that is,  $u_k = u(t_0)$  and  $v_k = v(t_0)$ .

In a matrix notation, Eq. (3-1) is rewritten as

$$d_k = Z_k' * Q Z_k \tag{4-2}$$

where ' and \* stand for the transpose and complex conjugate of the matrix.

The random variable for making binary decision based on all the  $L$  hops is then

$$D = \sum_{k=1}^L Z_k' * Q Z_k \tag{4-3}$$

We shall derive an expression for the probability of error given a particular transmitted signal and order of diversity  $L$ . Thus, assuming a Mark was transmitted during a particular data signaling interval, we shall compute

$$P(\text{error} | \text{mark}, L) = \Pr\{D < 0 | \text{mark}\} \tag{4-4}$$

To derive the statistical characteristics of the decision variable  $D$ , we first obtain the moment-generating function of decision variable  $D$ , that is,

$$M_D(s) = E\{\exp(sD)\} \tag{4-5}$$

where  $E\{\cdot\}$  means the ensemble average.

Since the matrix  $Q$  is Hermitian and  $E_Q$ , (3-3) is a Hermitian quadratic form, it is shown (12) that the moment-generating function of the  $k$ th hop decision variable  $d_k$  are assumed independent,

$$M_D(s) = \prod_{k=1}^L M_{d_k}(s) \tag{4-6}$$

From the literature (3), Eq. (4-14) reduces to

$$M_D(s) = \prod_{i=1}^2 \frac{\exp\{e_i z_i s/2(1-e_i s)\}}{(1-e_i s)^{L_i}} = M_{D,1}(s) \cdot M_{D,2}(s) \quad (4-7)$$

where  $e_i, i = 1, 2$  are the two real eigenvalues of the matrix  $K_z Q$

The probability density function of the decision variable  $D$  is then the inverse Laplace transform of Eq. (4-7).

Then, the probability density function is

$$F_D(x) = \int_{-\infty}^{\infty} P_1(y) P_2(y+x) dy \quad (4-8)$$

and the probability of error equivalent to Eq. (4-4) is

$$\begin{aligned} P(\text{error} | \text{mark}, L) &= \int_{-\infty}^0 F_D(x) dx \\ &= 1 - Q(a_1, a_2) + \frac{\exp\{-(a_1^2 + a_2^2)/2\}}{(1+a_3)^{2L-1}} \\ &\quad \sum_{m=0}^L I_m(a_1, a_2) \\ &= \sum_{k=m}^{L-1} \left( \frac{2L-1}{k-m} \right) \left\{ \left( \frac{a_1}{a_2 a_3} \right)^m a_3^k - (1 - \delta_{m0}) \right. \\ &\quad \left. \left( \frac{a_2 a_3}{a_1} \right)^m a_3^{2L-k-1} \right\} \quad (4-9) \end{aligned}$$

where  $\delta_{m0}$  is the Kronecker delta and

$$a_1^2 = \frac{z_1 a_3}{1+a_3}$$

$$a_2^2 = \frac{z_2}{1+a_3}$$

$$a_3 = \frac{e_1}{|e_2|}$$

and  $Q(\cdot, \cdot)$  is the Marcum's Q-function defined as

$$Q(a, b) = \int_b^{\infty} x \exp\{-(x^2 + a^2)/2\} I_0(ax) dx \quad (4-10)$$

For the covariance function or the "frequency-time" scattering function of the channel  $W(\tau, \mu)$ , we arbitrarily select the Gaussian-shaped function since there are no experimental data or specifications on it. The alternatives are the exponential or triangular-shaped function as shown in Fig. 5.

$$W(\tau, \mu) = 2\sigma^2 \frac{B_c}{B_f} \exp\left\{-\left(\frac{\mu}{B_f}\right)^2 - (\pi B_c \tau)^2\right\} \quad (4-11)$$

where  $\sigma^2$  is just equal to the average power received when a sinusoid of unity peak value is transmitted, and  $B_c$  and  $B_f$  are the correlation and fading bandwidth, respectively, equal to the frequency separation at which the correlation drops to  $1/e$  of its maximum value.

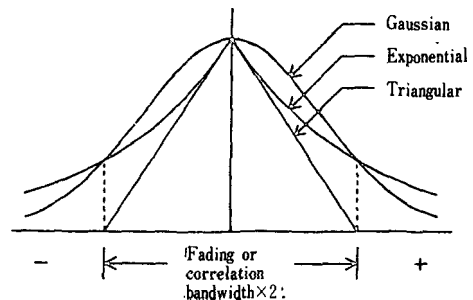


Fig. 5 Possible fading or correlation functions.

The average probability of error over the two adjacent data bits is then conditional on  $L, \theta_-,$  and

$$P(\text{error} | L, \theta_-, \theta_+) = \frac{1}{4} \sum_{a, b} P(\text{error} | L, a, b, \theta_-, \theta_+) \quad (4-12)$$

and over the random variable

$$P(\text{error} | L) = \frac{1}{4\pi^2} \iint_0^{2\pi} P(\text{error} | L, \theta_-, \theta_+) \cdot d\theta_- d\theta_+ \quad (4-13)$$

If the hopping pattern is mutually independent and identically distributed over the band which the signals can hop,

$$P(\text{error} | L) = \left( \frac{N-2}{N} \right)^2 P(\text{error} | L, f_{-1} \neq f_0, f_+ \neq f_0) + \frac{2(N-2)}{N^2} \{ P(\text{error} | L, f_- = f_0, f_+ \neq f_0) + P(\text{error} | L, f_- \neq f_0, f_+ = f_0) \} + \frac{4}{N^2} P(\text{error} | L, f_- = f_0, f_+ = f_0) \quad (4-14)$$

where  $N$  is the total number of hops in one code sequence period, and  $f_p$ ,  $p=-1, 0, +1$  are the hopping frequency of the pre-ceed-ceeding, present, and next hop, respectively.

## V. NUMERICAL RESULTS

The general expression for the probability of error is now calculated for a class of the fading channel. This is, we only consider in this section the cases when the channel is time-selective and the fading bandwidth of the channel is not greater than the inverse of one hop duration.

When the channel concerned is frequency-flat or purely time-selective, the cross-ambiguity functions are simply

$$A_1(\mu') = 2E \frac{\sin(\pi\mu')}{\pi\mu'} \quad (5-1)$$

$$A_0(\mu') = 2E \frac{\sin\{\pi(\mu' + 1)\}}{\pi(\mu' + 1)} \quad (5-2)$$

If we normalize the fading bandwidth to the hop rate, i.e.,

$$G = \frac{B_f}{1/T_h} \quad (5-3)$$

then the cross-covariance of random fading components becomes

$$K_{zm} = 2\sigma^2 \int_0^{T_h} A_1(\mu') A_m^*(\mu') \exp\left\{-\left(\frac{\mu'}{G}\right)^2\right\} d\mu' \quad (5-4)$$

And the parameters  $a_1$ ,  $a_2$ , and  $a_3$  in Eq. (4-9) can be determined with the normalized fading bandwidth and the power ratio of the scatter component to the specular component, and SNR the signal-to-noise ratio of the specular component to the white Gaussian noise.

When the normalized fading bandwidth is relatively small ( $G=0.1$ , as shown in Fig. 6), the diversity gain of a FFH-SS system increases rapidly with increasing the order of diversity  $L$ . And the order of diversity at which the performances over a Rayleigh channel are better than those over a Rician channel is 3. However, as is shown in Fig. 7, diversity gain decreases as the normalized fading bandwidth  $G$  increases, and the order of diversity at which the performances over a Rayleigh fading is superior to those over a Rician fading is now 4. Also, it can be shown that the system is not operated properly with no diversity ( $L=1$ ) or low order of diversity when  $G$  is large ( $G>0.5$ ). In Fig. 8, the error probabilities are shown for Rayleigh fading with the variations of the SNR and normalized fading bandwidth ( $G=0.3$  and  $0.6$ ). In this case, the error probabilities are roughly the same as those when the channel is Rician.

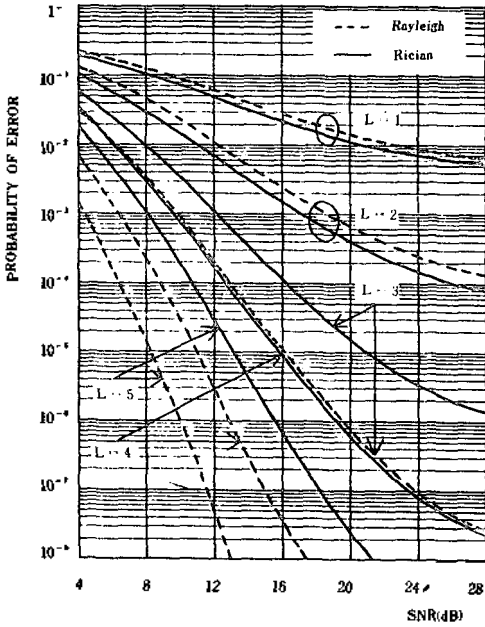


Fig. 6 Probability of Error for Rician ( $\gamma=0.2$ ) and Rayleigh Channel ( $G=0.1$ ).

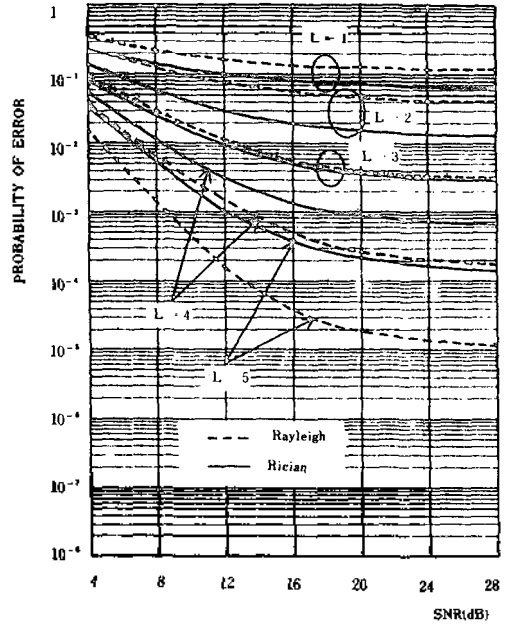


Fig. 7 Probability of Error for Rician ( $\gamma=1$ ) and Rayleigh Channel ( $G=0.5$ ).

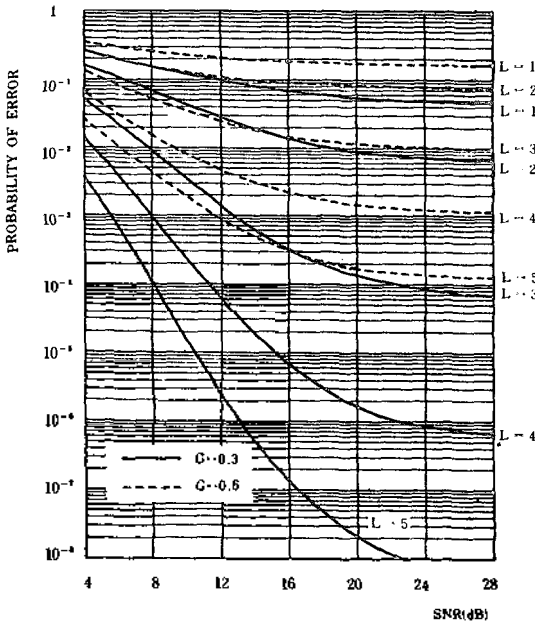


Fig. 8 Probability of Error for Rayleigh Channel ( $G=0.3$  and  $0.6$ ).

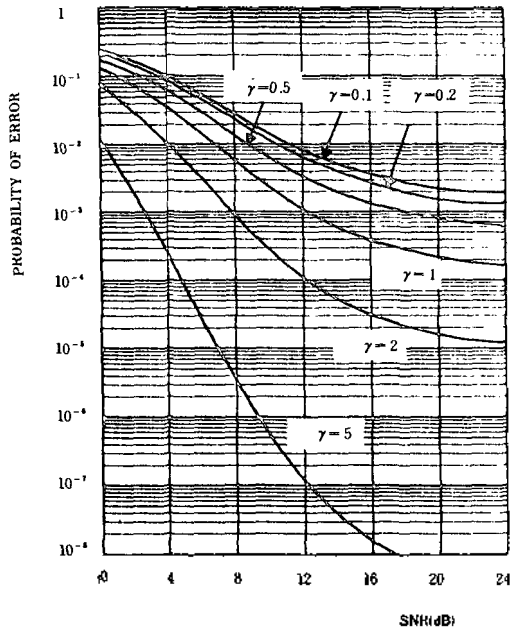


Fig. 9 Probability of Error when  $G=0.5$  and  $L=5$ .

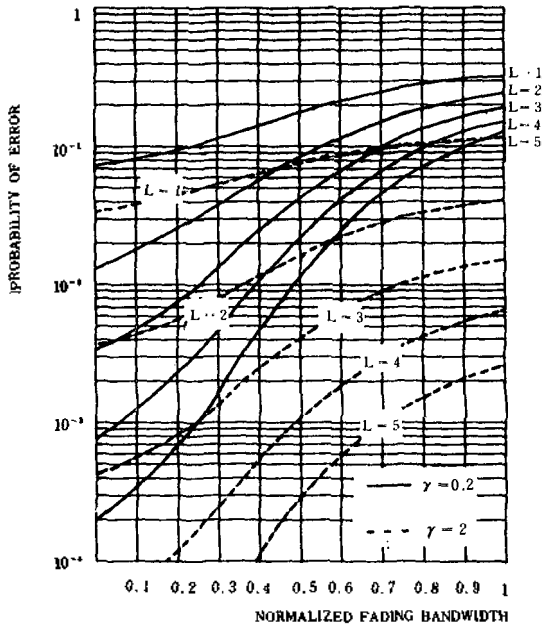


Fig. 10 Error Probabilities versus  $G$  ( $\gamma=0.2$  and 2, SNR = 10dB)

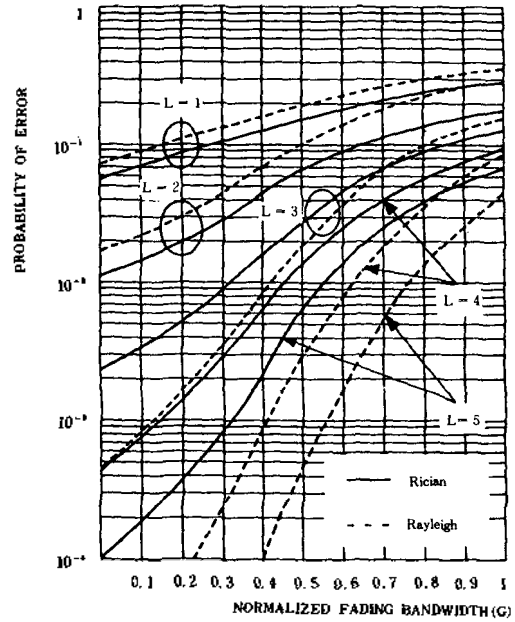


Fig. 11 Error Probabilities for Rician and Rayleigh Channel ( $\gamma=0.5$  and SNR=10 dB).

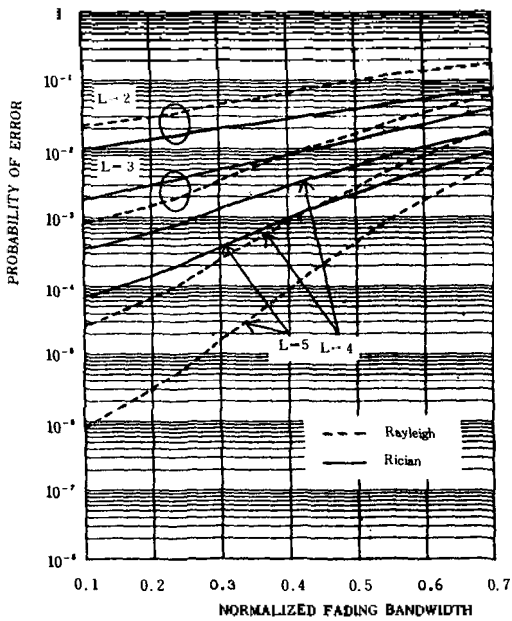


Fig. 12 Error Probabilities versus Normalized Fading Bandwidth ( $\gamma=1$ , SNR=10dB).

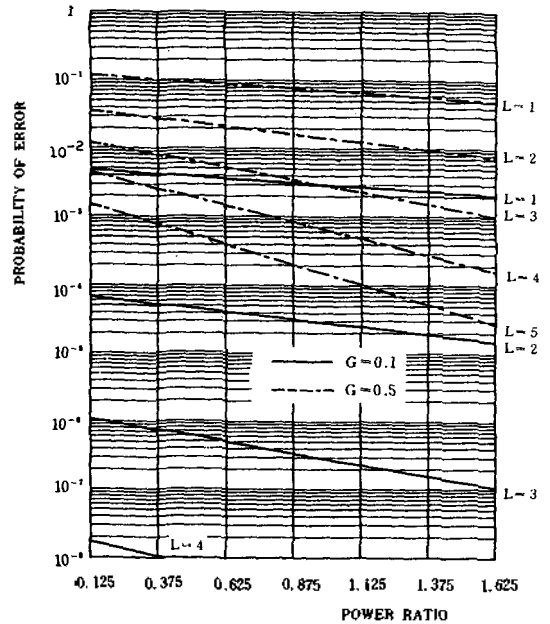


Fig. 13 Irreducible Error Rates versus Power Ratio ( $G=0.1$  and  $G=0.5$ ).



To see the effect of varying the relative amount of power in the scatter components of the received signal, Fig. 9 shows the probability of error for  $G=0.5$  and  $L=5$  when  $\gamma=0.1, 0.2, 0.5, 1, 2,$  and  $5$ . It can be seen from the figure that when the power ratio is small, increasing the relative power in the specular components does not significantly affect the system performance. On the other hand, when the  $\gamma$  is large, doubling the power ratio can result in marked improvement in system performance.

In Figs. 10, 11 and 12, the effect of varying the relative fading bandwidth to the hop rate are shown for the various order of diversity given  $SNR = 10$  (dB). The curves of Fig. 10 correspond to  $\gamma = 0.2, 2$ , those of Fig. 11 and 12 correspond to  $\gamma = 0$  (Rayleigh),  $0.5$  (Rician) and  $\gamma = 0, 1$ , respectively. As can be seen from Fig. 10, the diversity improvement decreases as the normalized fading bandwidth  $G$  increases, and is remarkable when the  $\gamma$  is small. In Figs. 11 and 12, the fact that the performance of the square-law combined over a Rayleigh channel is better than that over a Rician channel is shown as also shown in Figs. 6 and 7. For the order of diversity greater than 2, the normalized fading bandwidths at which this occur are approximately 0.7 for  $L=3$ , and greater than one for  $L=3$  and 5 in Fig. 11, and 0.4 for  $L=3$ , 0.66 for  $L=4$  and greater than one for  $L=5$  in Fig. 15.

Finally, the irreducible error probabilities over the power ratio  $\gamma$  are shown in Fig. 13 for  $G = 0.1$  and  $0.5$ . This figure shows the effect of fading alone on the probability of error.

## VI. CONCLUSIONS

An analysis of the performance of a binary noncoherent FFH-SS communication system

operating over a selective-Rician fading channel including a Rayleigh channel has been presented. Given the number of hops per data or alternatively the order of diversity, the average probability of error was determined, and the sensitivity of the error rate to such factors as the ratio of fading bandwidth to the hop rate, and relative amount of the received power in the scatter component of the selective channel to that in the specular component was investigated.

As the results of numerical calculation when the channel is time-selective, it was seen that the performance of a system is degraded rapidly with increasing the relative fading bandwidth, and there are no performance differences with the order of diversity as the normalized fading bandwidth increases. Also, for a given power in the scatter component, there are some fading bandwidth at which the performance of a system over Rayleigh fading channel is better than that over a Rician fading channel.

The expression for the probability of error presented in this paper is also applicable to the channel in which the more complicated channel impairments exist.

## REFERENCES

1. R.C. Dixon, Spread Spectrum Systems, John Wiley & Sons, New York, 1976.
2. G.R. Cooper and R.W. Nettleton, "A Spread-Spectrum Techniques for High-Capacity Mobile Communications," IEEE Trans. Veh. Technol., Vol. VT-27, pp.264-275, Nov. 1978.
3. C.S. Gardner and J.A. Orr, "Fading Effects on the Performance of a Spread Spectrum Multiple Access Communication System," IEEE Trans. Commu. Tech., Vol. COM-27, pp.143-149, Jan. 1979.

4. D.E. Borth and M.B. Pursley, "Analysis of Direct-Sequence Spread-Spectrum Multiple-Access Communication over Rician Fading Channels," IEEE Trans. Commu. Tech., Vol. COM-27, pp.1566-1577, Oct. 1979.
5. L.B. Milstein and D.L. Schilling, "The Effect of Frequency-Selective Fading on a Noncoherent FH-FSK System Operating with Partial-Band Tone Interference," IEEE Trans. Commu. Tech., Vol. COM-30, pp.904-912, May 1982.
6. E.A. Geraniotis and M.B. Pursley, "Error Probabilities for Slow Frequency-Hopped Spread-Spectrum Multiple-Access Communication over Fading Channels," IEEE Trans. Commu. Tech., Vol. COM-30, pp.996-1009, May 1982.
7. R.S. Kennedy, Fading Dispersive Communication Channels, Wiley, 1969.
8. P.A. Bellow, "Characterization of Randomly Time-Variant Linear Channels," IRE Trans. Commu. Syst. Vol. CS-11, pp.360-393, Dec. 1963.
9. R.A. Scholtz, et al, Special Issues on Spread Spectrum Communications, IEEE Trans. Commu. Technol., Vol. COM-25 August, 1977, COM-30, May, 1982.
10. S.W. Golomb, Shift Register Sequences, Holden-Fay, Inc., 1967.
11. P.A. Bello and B.D. Nelin, "The Influence of Fading Spectrum on the Binary Error Probabilities of Incoherent and Differentially Coherent Matched Filter Receivers," IRE Trans. Commu. Syst., Vol. CS-10, pp.160-168, June 1962.
12. P.A. Bello and B.D. Nelin, "Optimization of Sub-channel Data Rate in FDM-SSB Transmission over selectively Fading Media," IRE Trans. Commu. Syst., Vol. CS-12, pp.46-53, March 1964.